Received: 21 July 2020 | Revised: 1 December 2020 | Accepted: 5 December 2020

DOI: 10.1002/ardp.202000256

FULL PAPER

ARCH PHARM DPhG
Archiv der Pharmazie

Synthesis, in vitro cytotoxic and apoptotic effects, and molecular docking study of novel adamantane derivatives

Basak Turk-Erbul[1,2] | Ecem F. Karaman[3,4] | Gizem N. Duran[5] | Mehmet Ozbil[6] | Sibel Ozden[4] | Fusun Goktas[1]

[1]Department of Pharmaceutical Chemistry, Faculty of Pharmacy, Istanbul University, Istanbul, Turkey

[2]Department of Pharmaceutical Chemistry, Acibadem Mehmet Ali Aydinlar University, Istanbul, Turkey

[3]Department of Pharmaceutical Toxicology, Biruni University, Istanbul, Turkey

[4]Department of Pharmaceutical Toxicology, Istanbul University, Istanbul, Turkey

[5]Department of Chemistry, Marmara University, Istanbul, Turkey

[6]Institute of Biotechnology, Gebze Technical University, Kocaeli, Turkey

Correspondence
Fusun Goktas, Department of Pharmaceutical Chemistry, Istanbul University, Beyazıt, 34116 Istanbul, Turkey.
Email: fusung@istanbul.edu.tr

Funding information
Bilimsel Arastirma Projeleri Birimi, Istanbul Üniversitesi, Grant/Award Number: TYL-2017-25681

Abstract

[4-(Adamantane-1-carboxamido)-3-oxo-1-thia-4-azaspiro[4.4]nonan-2-yl]acetic acid (**4a**) and [4-(adamantane-1-carboxamido)-8-nonsubstituted/substituted-3-oxo-1-thia-4-azaspiro[4.5]decane-2-yl]acetic acid (**4b–g**) derivatives were synthesized; their structures were verified by elemental analysis, infrared spectroscopy, ^{1}H nuclear magnetic resonance (NMR), ^{13}C NMR, and mass spectroscopy data; and their in vitro cytotoxicity activities were investigated against human hepatocellular carcinoma, human prostate adenocarcinoma, and human lung carcinoma cell lines (HepG2, PC-3, and A549, respectively), and a mouse fibroblast cell line (NIH/3T3). All compounds, except compound **4e**, were found as cytotoxic, especially on A549 cells as compared with the other cells (selectivity index = 2.01–11.6). As a further step, the effects of compounds **4a–c** on apoptosis induction were tested and the expression of selected apoptosis genes was analyzed. Among the selected compounds, compound **4a** induced apoptosis remarkably. Moreover, computational calculations of the binding of compounds **4a–c** to the BIR3 domain of the human inhibitor of apoptosis protein revealed ligand–protein interactions at the atomistic level and emphasized the importance of a hydrophobic moiety on the ligands for better binding.

KEYWORDS
antitumor activity, cytotoxic activity, structure elucidation, synthesis, thiazolidine

1 | INTRODUCTION

Cancer is one of the leading causes of death worldwide today.[1] Whereas cancer can be caused due to a genetic change in which a normal cell is transformed into a malignant cell, cell death escaping is one of the fundamental changes in a cell that leads to this malignant transformation.[2] Drug resistance in cancer treatment is an important factor among all the factors, leading to ultimate failure. Apoptosis or programmed cell death is defined by morphological change that causes internal and external nonpathological cell loss. Apoptosis occurs spontaneously in malignant tumors and often slows down growth. The role of apoptosis in cancer development has recently become more attractive for oncologists. Antiapoptotic properties or resistant cell death has been proposed as a sign of cancer, so induction of apoptosis is thought to be a popular strategy for killing cancerous cells.[3–6] Therefore, loss of apoptosis provides a survival advantage to tumor cells and leads to resistance of cancer cells for anticancer therapies.[2]

The adamantane and 4-thiazolidinones rings are crucial components of bioactive molecules. After the discovery of amantadine as an antiviral and antiparkinson drug, thousands of adamantane derivatives were synthesized and tested for biological activities.[7] Up until today, the studies have shown that adamantane derivatives exhibit various pharmaceutical effects including antiviral,[8–11] anticancer,[12] antibacterial,[13,14] antifungal,[15,16] anti-inflammatory,[17,18] trypanocidal,[19] antiparkinson,[20,21] and 11β-HSD1 inhibitory activities.[22,23] Moreover, besides amantadine, some drug molecules containing adamantyl ring are

also known, such as adapromine, rimantadine, vildagliptin (antiviral), saxagliptin, tromantadine (antidiabetic), adapalene (treatment of acne), bromantane (anxiolytic), memantine (Alzheimer's disease) with their various pharmacological effects (Figure 1).[24–28] When adamantane is bound to the scaffold of various structures, this adamantyl moiety increases the cytotoxic effect of the molecule due to its possible lipophilic character or unique structure.

However, homologs of 2-alkyl/aryl-substituted 4-thiazolidinones, namely spirothiazolidinones, are one of the most studied heterocyclic systems that show a wide range of biological activities such as antibacterial,[29,30] anticancer,[31,32] antifungal,[33] and antiviral activities.[34]

In light of recent studies about the antitumor, antiproliferative, or anticancer effects of compounds bearing adamantane ring,[35–40] our aim is to synthesize several novel spirothiazolidinone compounds

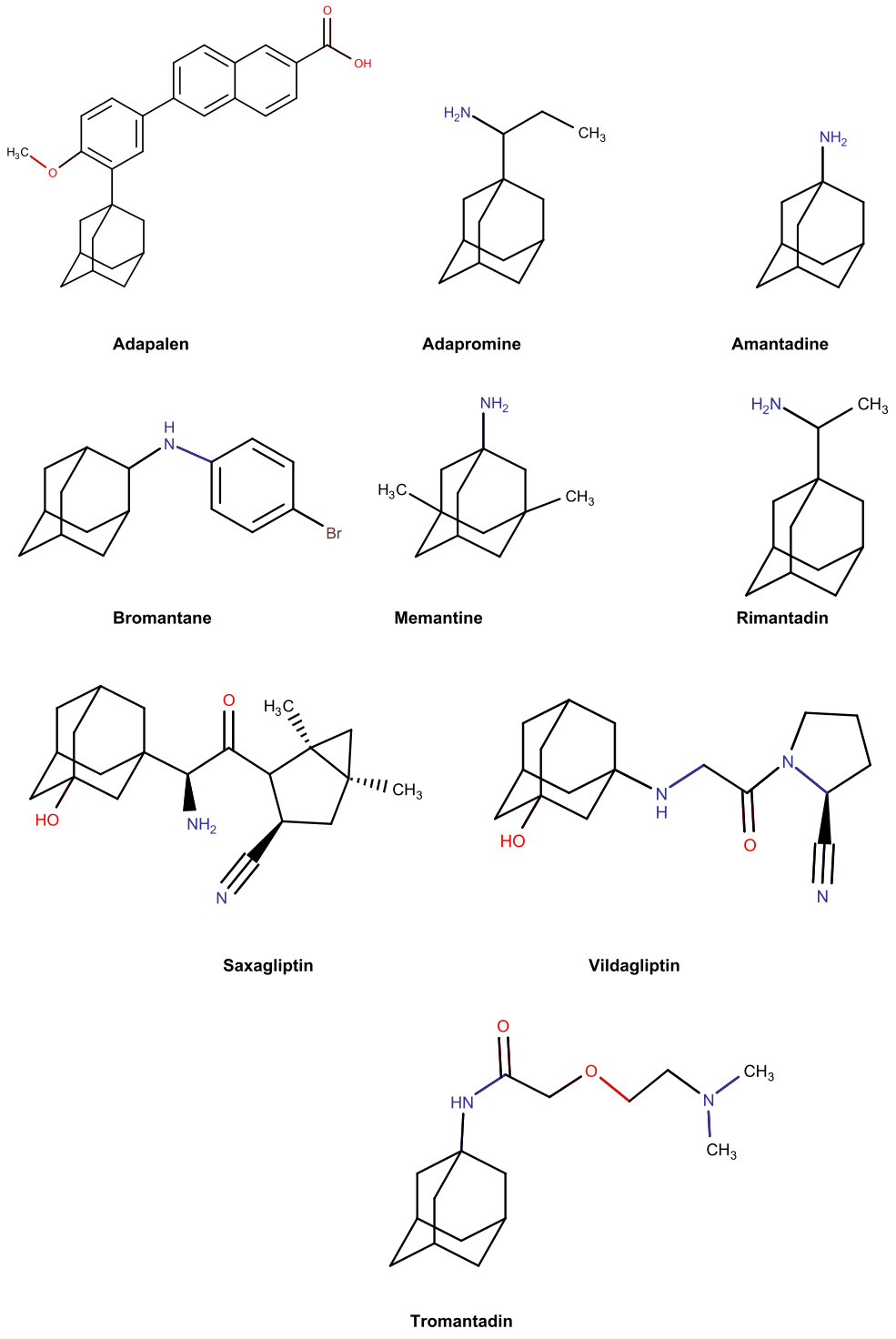

FIGURE 1 Some drug molecules containing the adamantane ring

bearing adamantane ring (Scheme 1). The structures of all obtained products were elucidated by spectroscopic methods and were screened for their in vitro cytotoxic activity against HepG2, PC-3, A549, and NIH/3T3 cell lines. Furthermore, the effects of compounds **4a–c** on apoptosis induction were tested and supported with gene expression results and molecular docking calculations. This investigation can lead to further design and development of molecules as antitumor agents.

2 | RESULTS AND DISCUSSION

2.1 | Chemistry

The synthesis of the target compounds is shown in Scheme 1. Methyl adamantane-1-carboxylate (**2**) was synthesized by adamantane-1-carboxylic acid (which is commercially available) in the presence of methanol and 98% H_2SO_4. The methyl ester (**3**) was obtained with the reaction of excess hydrazine hydrate under reflux for 15 h without using any solvent. With the addition of cyclopentanone/cyclohexanone/substituted cyclohexanone compounds in adamantane-1-carbohydrazide, **3** was cyclized with mercaptosuccinic acid in absolute toluene and the desired derivatives **4a–g** were obtained via one-pot synthesis. Moreover, the synthesized compounds were characterized via analysis of IR, ^{1}H nuclear magnetic resonance (NMR), ^{13}C NMR (proton decoupled), ^{13}C NMR (distortions enhancement by polarization transfer [DEPT]), 2D-NMR (heteronuclear single-quantum coherence [HSQC]), and mass spectroscopy (MS). The atomic numbering of obtained products applied for NMR analysis is shown in Figure 2.

The IR spectra of compounds **4a–g** demonstrated common characteristic absorption bands at 3496–3111 cm^{-1} (O–H/N–H), 1707–1616 cm^{-1} (HO–C=O) 1697–1690 cm^{-1} (C=O), and 1668–1663 cm^{-1} (NH–C=O), which provide the evidence for the

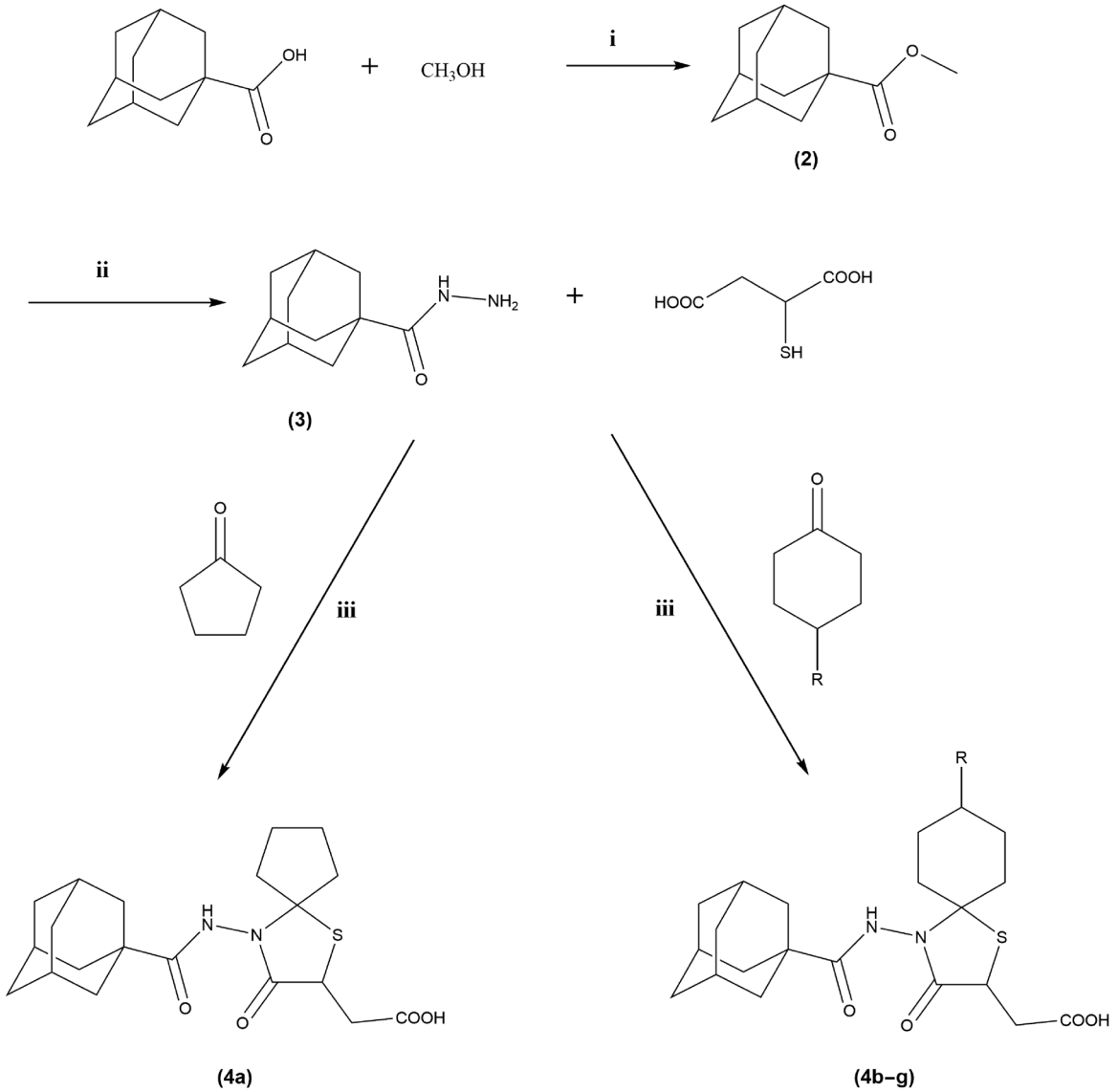

SCHEME 1 The synthesis pathway of compounds **4a–g**. Compounds: **4b**: R = H; **4c**: R = CH_3; **4d**: R = C_2H_5; **4e**: R = C_3H_7; **4f**: R = $C(CH_3)_3$; **4g**: R = C_6H_5. Reagents and conditions: (i) H_2SO_4, 75°C, 3 h; (ii) hydrazine hydrate, 150°C, 15 h; (iii) anhydrous toluene, 120°C, 16 h

cycloaddition reaction between azomethine intermediates and mercaptosuccinic acid.

In the ^{1}H NMR spectra of the compounds, –COOH and –CONH protons were observed as a singlet at about σ: 12.63–12.54 ppm (1H) and σ: 9.67–9.59 ppm (1H), respectively. The ^{1}H NMR spectra of compounds **4a**–**g** displayed doublet of doublets attributed to ($SCHCH_2$) methine ring protons at 2-position of the 4-thiazolidinone system at about σ: 4.06–3.99 ppm (1H). In the ^{1}H NMR spectra of compound **4e**, $-CH_2COOH$ protons were observed as a doublet of doublets at about σ: 3.01 ppm (1H) and σ: 2.46 ppm (1H).

The same resonance spectra of compounds **4a**–**c**, **4d**, and **4f** were observed at about σ: 3.05–3.01 ppm (1H, dd) and σ: 2.49–2.41 ppm (5H, m, with dimethyl sulfoxide [DMSO]-d_6). The ^{1}H NMR spectra of compounds **4a**–**f** showed the resonance of the $C_{2'}$, $C_{8'}$, and $C_{10'}$ protons of adamantane ring at σ: 1.85–1.84 ppm (6H, d) and the resonance of the $C_{4'}$, $C_{6'}$, and $C_{9'}$ protons of adamantane ring at σ: 1.81–1.60 ppm (m, with 4-thiazolidinone ring protons). Furthermore, protons that belong to $C_{3'}$, C_5, and $C_{7'}$ bridgehead carbons are observed as broad singlet values of 3H integral at δ 1.98–2.01 ppm in a lower field due to the W effect, compared with other protons connected to adamantane. In the ^{13}C NMR spectra of compounds **4a**–**g**, the thiazolidinone C_2 carbon (σ: 40.49–40.48, with DMSO-d_6), thiazolidinone C═O carbon (σ: 172.23–172.15 ppm), and thiazolidinone C_5 carbon (σ: 74.80–71.02 ppm) peaks verified the formation of desired spirothiazolidinone structures. Observed peaks of acid C═O carbon (σ: 176.92–176.80 ppm), amide C═O carbon (σ: 168.66–168.57 ppm), and $-CH_2COOH$ methylene carbon (σ: 39.30–39.21 ppm) in the ^{13}C NMR spectra supported the cycloaddition reaction. The ^{13}C NMR (DEPT) spectrum of compound **4b** is also supported by a related interpretation. Moreover, 2D-NMR (HSQC) experiment was performed to establish the interfragment relationship and assign the proton and carbon signals of the prototype compound **4c**. HSQC (^{1}H-^{13}C) experiment of representative **4c** also confirmed the structure. In mass spectra of **4a**, **4c**, **4d**, and **4f**, $[M-H]^-$ molecular ion peaks were observed in the negative ionization mode, whereas in the positive mode, all characteristic *m/z* 135 peaks of adamantane were common.

2.2 | Pharmacology/biology

2.2.1 | Assessment of cytotoxicity

The cytotoxic activity of compounds was studied using the MTT (3-(4,5-dimethylthiazol-2-yl)-2,5-diphenyltetrazolium bromide) assay. HepG2, PC-3, A549, and NIH/3T3 cells were exposed to a broad range of compound concentrations for 24 h. The results of this experiment and IC_{50} values of compounds are shown in Table 1. According to these results, compounds **4a**, **4b**, and **4c** showed a quite high cytotoxic activity with average IC_{50} values of 0.15, 0.23, and 0.22 mM, respectively in A549 cells, whereas they exhibited the weakest cytotoxic effect in NIH/3T3 cells. The cytotoxic activities of the compounds in cell lines were less potent when compared with doxorubicin. It has been observed that A549 cells were more sensitive for cytotoxic activity among these cell lines. According to our results, we selected compounds **4a**–**c** for further analysis in A549 cells.

2.2.2 | The effects of compounds 4a, 4b, and 4c on apoptosis induction

We tested the ability of **4a**–**c** to induce apoptosis by a flow cytometry analysis in A549 cells. The cytograms of bivariate annexin V/propidium iodide (PI) analysis of A549 cells after treatment with **4a**–**c** are shown in Figure 3. Apoptosis induction was detected at the rates of 68.86%, 35.04%, and 55.48%, respectively.

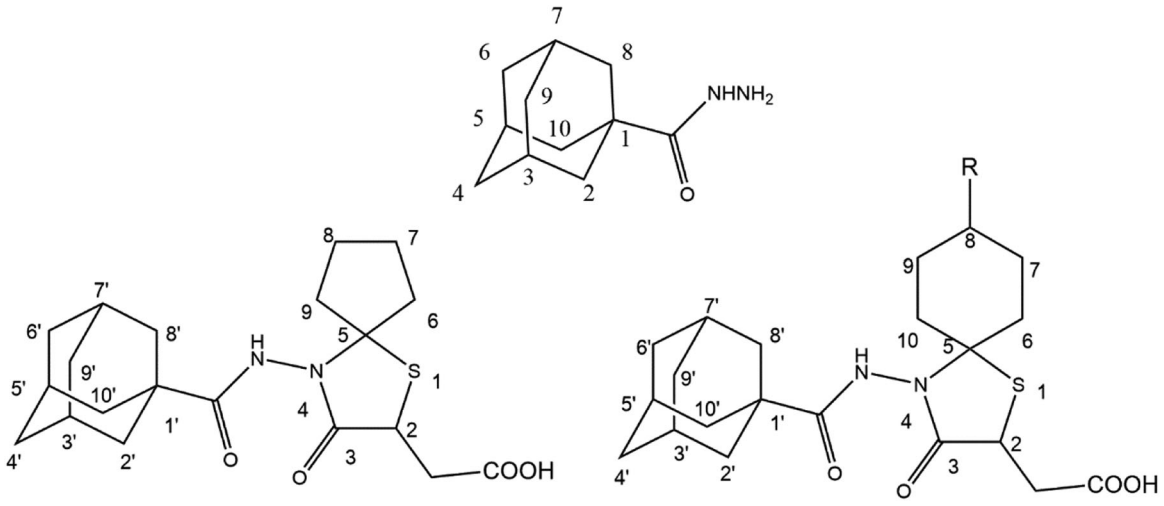

FIGURE 2 Atomic numbering of obtained products applied for nuclear magnetic resonance analysis

TABLE 1 IC_{50} (mM) values of the substances obtained by using the MTT test in cancerous and healthy cells

Compound	PC-3		HepG2	
	IC_{50}[a]	SI[b]	IC_{50}[a]	SI[b]
4a	nd (>2.55)	nd	2.52 ± 0.1	0.679
4b	0.41 ± 0.003	**5.86**	**0.53 ± 0.05**	**4.55**
4c	1.24 ± 0.05	0.85	1 ± 0.06	1.06
4d	1.08 ± 0.01	0.54	0.51 ± 0.03	1.13
4e	0.45 ± 0.01	1.31	0.57 ± 0.02	1.04
4f	0.66 ± 0.02	1.06	0.37 ± 0.03	1.88
4g	0.54 ± 0.02	1.31	0.31 ± 0.01	**2.33**
Doxorubicin	**0.025 ± 0.005**	**2.12**	**0.051 ± 0.01**	**1.04**
Compound	**A549**		**NIH/3T3**	
	IC_{50}[a]	SI[b]	IC_{50}[a]	
4a	**0.15** ± 0.01	**11.6**	1.71 ± 0.08	
4b	**0.23** ± 0.02	**10.32**	2.42 ± 0.08	
4c	**0.22** ± 0.02	**4.77**	1.06 ± 0.05	
4d	0.24 ± 0.01	**2.41**	**0.58 ± 0.03**	
4e	**0.48 ± 0.02**	**1.22**	**0.59 ± 0.05**	
4f	0.35 ± 0.024	**2.01**	**0.7 ± 0.03**	
4g	**0.28 ± 0.02**	**2.58**	**0.71 ± 0.03**	
Doxorubicin	**0.014 ± 0.003**	**3.79**	0.053 ± 0.007	

Note: Boldface shows that high cytotoxic activity.

Abbreviations: MTT, 3-(4,5-dimethylthiazol-2-yl)-2,5-diphenyltetrazolium bromide; nd, not determined.

[a]IC_{50} = 50% cytotoxic concentration against in vitro tested cells. Data are presented as mean ± *SD*.

[b]SI = selectivity index—IC_{50} value relative to a normal cell.

2.2.3 | The effects of compounds 4a, 4b, and 4c on apoptosis genes

To support our findings, we analyzed the gene expression of selected apoptosis genes (*p53*, *CASP3*, *CASP9 BCL2*, *B*, *CYCS*, *AIF*, *APAF1*, and *XIAP*) to investigate the potential apoptotic effects of compound **4a–c**. In Figure 4a–c, our data showed that although all compounds altered expression levels of apoptosis genes significantly, exposure to compound **4a** induced apoptosis more effectively. Expression levels of *p53* (1.4-fold), *CASP3* (1.6-fold), *BAX* (4.05-fold), *CYCS* (4.42-fold), and *AIF* (2-fold) were upregulated and expression levels of *CASP9* (2.3-fold), *BCL2* (12.5-fold), and *XIAP* (5-fold) were downregulated after **4a** treatments. Besides, the *APAF1* gene expression did not change as compared with the control group.

The newly synthesized compounds were tested for their ability to inhibit metabolic activity as an indicator for the viability of cancerous and noncancerous cell lines. First, the compounds were tested for their ability to inhibit the viability of HepG2, PC-3, A549, and NIH/3T3 cell lines using the MTT assay. According to IC_{50} values, compounds were shown to exhibit the most cytotoxic effect on A549 cell line among cancerous cell lines. Among cancerous cell lines, the most cytotoxic compounds were **4a**, **4b**, and **4c** for A549 in terms of IC_{50} values. After exposure to these compounds, the viability of noncancerous cell line, NIH/3T3, was not generally affected by these compounds. Similar to our results, Ali et al.[6] observed that the designed new adamantane derivatives exhibited the lowest IC_{50} concentrations in A549 cells according to the MTT assay.

According to the MTT results, **4a**, **4b**, and **4c** were selected to assess the induction of apoptosis in A549 cells by a flow cytometer. Among the selected compounds, **4a** and **4c** induced apoptosis significantly at IC_{50} levels.

It has been reported that many approved cancer treatments could affect via the intrinsic pathway.[41] The intrinsic pathway (or mitochondrial one) is regulated by *BCL2* proteins that lead to the release of apoptogenic factors and cause the formation of the apoptosome, including apoptotic protease-activating factor-1 (*APAF1*), cytochrome-*c*, and caspase 9.[42] *p53* is one of the best known tumor suppressor proteins, and besides the induction of apoptosis, it is involved in cell cycle regulation, development, differentiation, gene amplification, and cellular senescence.[2] Activated *p53* can induce apoptotic cell death through both the extrinsic and intrinsic pathways.[2,43] The elevated *BAX*/*BCL2* ratio is regarded as a sign of apoptosis and indicates

mitochondrial dysfunction, which leads to the release of cytochrome-*c* (*CYCS*). Moreover, this sequential cascade triggers several proteases including caspase-1, -3, and -9.[44-46] Caspase-3 (*CASP3*) also activates the pathway of several enzymatic events and serves as the promoter of apoptosis.[47] In the present study, compounds **4a** and **4c** induced *p53* and *BAX* gene expression and decreased expression levels of *BCL2*; however, the *BAX*/*BCL2* ratio was higher after compound **4a** exposure. As a result of this, *CYCS* and *Cas3* gene expression levels were significantly upregulated after compound **4a** exposure, whereas *CASP3* and *CASP9* were downregulated after compound **4c** exposure in A549 cells. Ali et al.[6] have showed upregulation of *p53*, *BAX*, and *CASP3* and downregulation of *BCL2* in A549 cells after new adamantane derivative exposure. We measured the expression levels of *APAF1*, apoptosis-inducing factor (*AIF*), and X-linked inhibitor of apoptosis protein (*XIAP*) genes as well. *XIAP* is one of the inhibitors of apoptosis proteins (IAPs), which blocks the caspase activities.[48]

After exposure of compound **4a**, expression levels of *AIF* increased and *XIAP* levels decreased, whereas the *APAF1* expression level did not change. Related with flow analysis, histograms were also supported with our gene expression results.

2.3 | Molecular docking

In the cytotoxic activity and gene expression test results, compounds **4a**–**c** were determined as the most potent and promising antitumor agents. IAPs are a family of main apoptosis regulators and *XIAP* (X-chromosome-linked IAP) is known as the best-characterized IAP member.[6,43,49] Therefore, molecular modeling studies were performed against *XIAP* (PDB ID: 1G73) protein. 2D interaction schemes and 3D binding poses are demonstrated in Figures 5 and 6, respectively. All interactions are listed in Table 2. As it can be seen from the table, compounds **4a** and **4c** interacted with XIAP mostly through hydrophobic interactions and compound **4b** interacted with a mixture of hydrophobic and hydrophilic interactions.

IAPs are a family of apoptosis regulators that were upregulated in various cancer cells. Overexpressions of these proteins maintain the proliferation of cancer cells and bypassing to several therapeutics for cancer.[50] In addition, XIAP has been highly reported to be overexpressed in lung cancer, causing inhibition of apoptosis and treatment resistance.[51,52] Therefore, molecular perspective into XIAP, which is one of the therapeutic targets for cancer, will be valuable for the development of drugs for cancer treatment. Our study considered that **4a**–**c** could be used as a novel potential monovalent Smac mimetic due to their high affinity of binding with XIAP which may exhibitthe profile of an XIAP antagonist. As can be seen from the gene expressions results, decreasing XIAP expression levels could lead to an increased caspase activity, inducing apoptosis. Hence, antiapoptotic effects of XIAP have also been decreased due to their cellular amount reduction, leading to activation of apoptotic genes such as *p53*, *CASP3*, *BAX*, and *CYCS*. Hence, this could be the reason that compounds **4a**–**c** showed a remarkable cytotoxicity against lung cancer cells A549. Due to the promising biological activities of **4a**–**c**, we also performed the screening of novel compound candidates for their apoptotic activity and affinity to XIAP, and it could be suggested that they had potentials for lung cancer treatment.

3 | CONCLUSION

The novel adamantyl-substituted spirothiazolidinone derivatives were successfully synthesized in the presented study. The structures were enlightened and confirmed by instrumental techniques. As a result of the biological assay, all compounds (except for compound **4e**) show a selective cytotoxic effect, especially on the A549 cell line. Compound **4a** triggered apoptosis more effectively than other compounds, which is consistent with gene expression results.

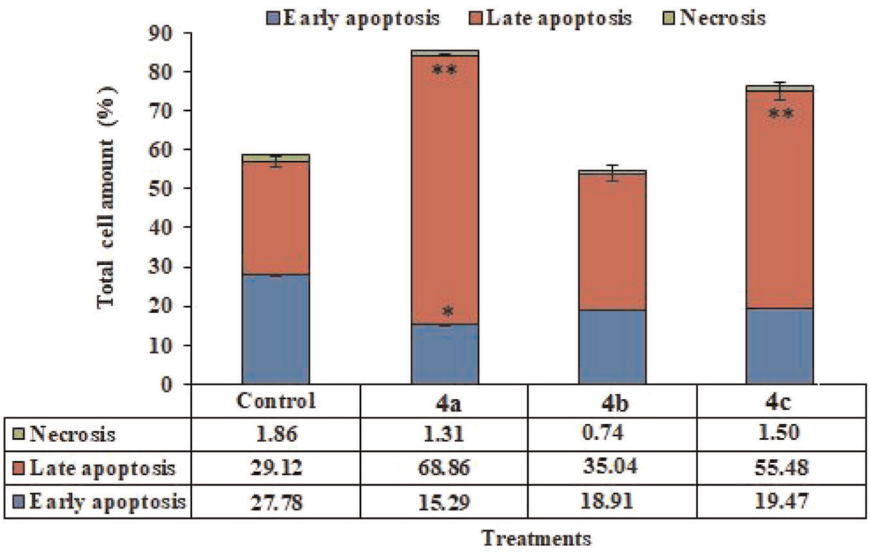

FIGURE 3 Effects of the selected compounds (at IC_{50} concentrations) on apoptosis in A549 cells after 24-h exposure determined by staining with Annexin V/propidium iodide. Data are presented as mean ± *SD*. Statistical analysis was performed by analysis of variance + Dunnett's post-hoc test. Statistically significant changes are indicated by $^{*}p < .05$; $^{**}p < .001$

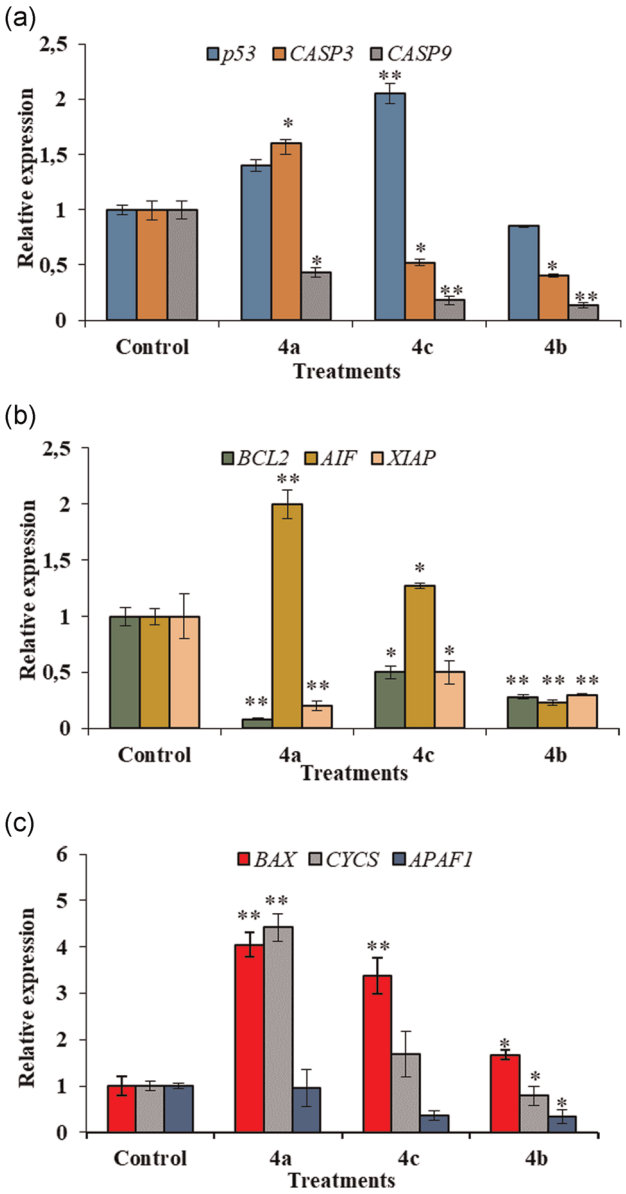

FIGURE 4 Effects of the selected compounds (at IC_{50} concentrations) on relative gene expressions (a–c) in A549 cells after a 24-h exposure. Data are presented as mean ± *SD*. Statistical analysis was performed by analysis of variance + Dunnett's post-hoc test. Statistically significant changes are indicated by $^{*}p < .05$; $^{**}p < .001$

These findings indicated that compound **4a** could show its antitumor activity through the induction of apoptosis via intrinsic pathway in A549 cells. According to the computational calculations, although compound **4a** seemed to have the lowest binding affinity, the difference of 0.5 kcal/mol does not make the binding less favorable. Therefore, it is revealed that all three ligands (**4a**–**c**) bound to similar binding pockets with similar binding affinities, making them all possible drug candidates. Overall, these observations can provide a promising framework for further design and development of adamantane-based compounds with a potential antitumor activity.

4 | EXPERIMENTAL

4.1 | Chemistry

4.1.1 | General

Reagents, starting materials, and solvents were purchased from Merck and Sigma-Aldrich. Melting points (mp) were recorded on a Büchi Melting Point B-540 device and are uncorrected. ^{1}H and ^{13}C NMR spectra were obtained by Varian UNITY INOVA 500 MHz NMR, using DMSO-d_6 as a solvent and tetramethylsilane (TMS) as internal standard. 2D-NMR experiments (HSQC) and DEPT ^{13}C NMR were performed for the interpretation of novel synthesized compounds. The atoms of target compounds were numbered for the interpretation by NMR, as shown in Figure 1. Atmospheric pressure chemical ionization (APCI) MS was carried out using an Advion Expression Compact Mass Spectrometer. Elemental analyses (C, H, N) were performed by Thermo Finnigan Flash EA 1112 Series device. To monitor the reaction during the synthesis and to check the purity of the compounds, thin-layer chromatography was performed using Merck pre-coated with silica gel 60 F_{254} aluminum sheets (layer thickness 0.25 mm) and the spots were visualized with the help of Dragendorff reagent.

The original spectra are provided as Supporting Information. The InChI codes of the investigated compounds, together with some biological activity data, are also provided as Supporting Information.

4.1.2 | Synthesis of methyl adamantane 1-carboxylate (2)[53]

For synthesis, 98% H_2SO_4 (8 ml) was added dropwise into a stirred solution of adamantane-1-carboxylic acid (9 g, 0.05 mol) in methanol. The mixture was heated under reflux for 3 h. During cooling, the mixture was poured over crushed ice (250 g). Precipitated crystals were washed with water and 10% $NaHCO_3$ subsequently. Solid crystals were allowed to dry. Light yellow solid; yield: 90%; mp: 35–36°C; IR υ_{max} (cm^{-1}): 2927, 2850 (C–H), 1732 (C═O); 1450, 1425 (C–H); 1238 (C–O).

4.1.3 | Synthesis of adamantane 1-carboxylic acid hydrazide (3)[54]

The mixture of methyl adamantane-1-carboxylate (**2**; 9.7 g, 0.05 mol) and excess 98% hydrazine hydrate (15 ml) was stirred under reflux for 15 h. During cooling, chilled water (150 ml) was added to the mixture and the separated solid white crystal was filtered off, washed with cold water, dried, and crystallized from water. White crystals; yield: 81%; mp: 147–148°C; IR (KBr) υ (cm^{-1}): 3332, 3275 (N–H); 2908, 2848 (C–H); 1616 (C═O); 1521 (N–H); 1456, 1367 (C–H). ^{1}H NMR (500 MHz) (DMSO-d_6) δ (ppm): 1.63 (6H, 2d,

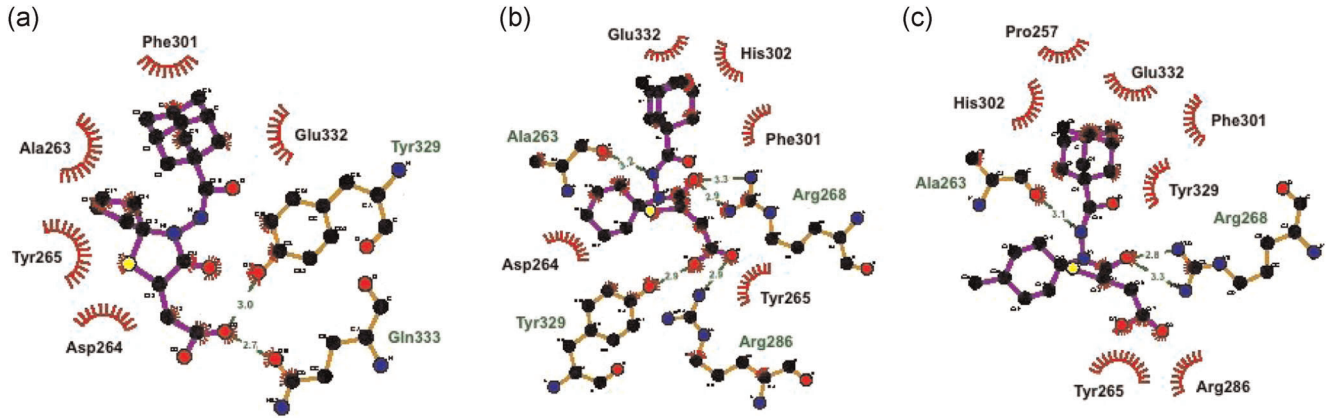

FIGURE 5 2D interaction schemes for compounds (a) **4a**, (b) **4b**, and (c) **4c**. H-bonding amino acids are represented by green, H-bonds by dotted lines, and hydrophobic interaction amino acids are written in black and represented by red half circles

J = 11.7 Hz, adm. C_4–H/C_6–H/C_9–H); 1.75 (6H, d, J = 2.7 Hz, adm. C_2–H/C_8–H/C_{10}–H); 1.94 (3H, broad s, adm. C_3–H/C_5–H/C_7–H); 4.10 (2H, s, NH_2); 8.67 (1H, s, CONH). ^{13}C (HSQC) NMR (500 MHz) (DMSO-d_6) δ (ppm): 28.02/28.05/28.11 (3H, adm. C_3/C_5/C_7); 36.53/36.61/36.68 (adm. C_4/C_6/C_9); 38.98/39.05/39.12 (adm. C_2/C_8/C_{10}); 39.49 (adm. C_1); 176.77 (CONH).

4.1.4 | General procedure for the synthesis of spirothiazolidinone derivatives bearing the adamantine ring (4a–g)

Cyclopentanone/4-(substituted/substituted) cyclohexanone compound (0.015 mol) was added into the solution of adamantane 1-carboxylic acid hydrazide (0.005 mol) in 30 ml of anhydrous toluene. The reaction mixture was heated under reflux using a Dean–Stark trap for 2 h. After adding 2-mercaptosuccinic acid (0.015 mol), the reaction mixture was heated for a further 13–14 h. Anhydrous toluene was removed under reduced pressure and the excess acid was neutralized with a saturated sodium bicarbonate solution. After cooling, the product formed was filtered off, washed with water, and purified by crystallization from the appropriate solvent.

*[4-(Adamantane-1-carboxamido)-3-oxo-1-thia-4-azaspiro[4.4] nonan-2-yl]acetic acid (**4a**)*

Brown crystals; yield: 74%; mp: 143°C; IR: 3543, 3241 (O–H/N–H); 2907, 2851 (C–H); 1705, 1694, 1668 (C=O); 1454, 1368 (C–H); 1246 (N–H and C–N). ^{1}H NMR (DMSO-d_6, 500 MHz) δ (ppm): 1.57–1.63 (4H, m, C_7–H/C_8–H), 1.63–1.78 (8H, m, C_{6-9}–H (ax.), adm. C_4'–H, C_6'–H/C_9'–H); 1.84 (6H, d, J = 2.7 Hz, adm. C_2'–H/C_8'–H/C_{10}'–H); 1.98 (3H, broad s, adm. C_3'–H/C_5'–H/C_7'–H); 2.06–2.28 (2H, m, C_{6-9}–H (eqv.)); 2.49 (5H, m, with DMSO-d_6 –CHa–COOH); 3.01 (1H, dd, J = 16.9; 4.0 Hz, –CHb–COOH) 4.05 (1H, dd, J = 10.4; 4.0 Hz, C_2–H); 9.59 (1H, s, CONH); 12.56 (1H, s, COOH). ^{13}C NMR (DMSO-d_6, 500 MHz) δ (ppm): 23.30 (cyclopentilidene C_7/C_8); 27.94/27.97 (adm. C_3'/C_5'/C_7'); 36.38/36.45/36.52 (adm. C_4'/C_6'/C_9'); 38.68 (cyclopentilidene C_6/C_9); 38.77/38.82/38.88 (adm. C_2'/C_8'/C_{10}'); 40.26 (C_1'); 40.48 (DMSO-d_6 and C_2); 39.00 (CH_2–COOH); 74.80 (cyclopentilidene C_5); 168.58 (CONH); 172.15 (C_3); 176.80 (COOH); anal. calcd. for $C_{20}H_{28}N_2O_4S{\cdot}H_2O$: C, 58.51; H, 7.37; N, 6.82. Found: C, 58.47; H, 7.07; N, 6.70.

*[4-(Adamantane-1-carboxamido)-3-oxo-1-thia-4-azaspiro[4.5] decan-2-yl]acetic acid (**4b**)*

White powder; yield: 41%; mp: 156–158°C; IR: 3465, 3115 (O–H/N–H); 2905, 2851 (C–H); 1707, 1690, 1666 (C=O); 1520 (N–H);

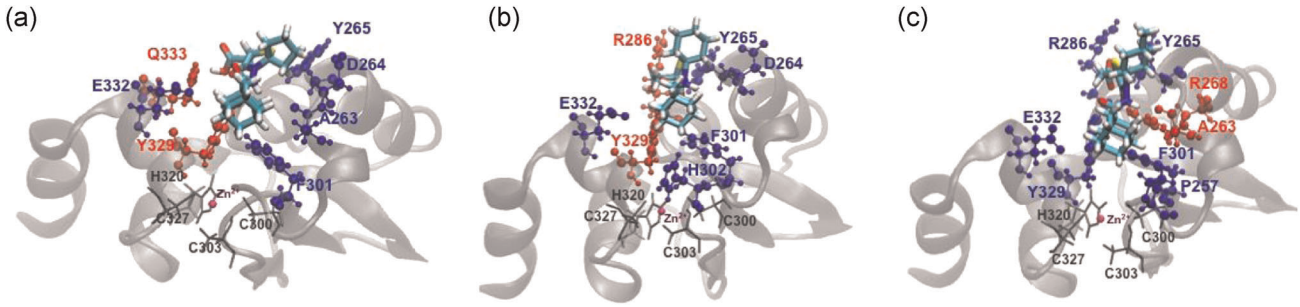

FIGURE 6 Binding sites for compounds (a) **4a**, (b) **4b**, and (c) **4c**. Hydrophobic amino acids are represented by blue, hydrophilic residues by red, ligand carbon atoms by cyan, and hydrogen atoms by white. Structural Zn^{2+} ion is represented by a purple sphere

TABLE 2 Binding sites for compounds **4a**, **4b**, and **4c** with interaction types for each amino acid on XIAP-BIR3 and binding affinities on each site are provided

Compound	Interacting residues	Interaction type	Binding affinity (kcal/mol)
4a	Ala263	Hydrophobic	−6.9
	Asp264	Hydrophobic	
	Tyr265	Hydrophobic	
	Phe301	Hydrophobic	
	Tyr329	H-bonding	
	Glu332	Hydrophobic	
	Gln333	H-bonding	
4b	Ala263	H-bonding	−7.2
	Asp264	Hydrophobic	
	Tyr265	Hydrophobic	
	Arg268	H-bonding	
	Arg286	H-bonding	
	Phe301	Hydrophobic	
	His302	Hydrophobic	
	Tyr329	H-bonding	
	Glu332	Hydrophobic	
4c	Pro257	Hydrophobic	−7.4
	Ala263	H-bonding	
	Tyr265	Hydrophobic	
	Arg268	H-bonding	
	Arg286	Hydrophobic	
	Phe301	Hydrophobic	
	His302	Hydrophobic	
	Tyr329	Hydrophobic	
	Glu332	Hydrophobic	

1446, 1369 (C–H); 1249 (N–H and C–N). ^{1}H NMR (DMSO-d_6, 500 MHz) δ (ppm): 0.98–1.05 (1H, broad q, sty.C_8-ax-H); 1.32–1.43 (2H, m, sty.C_{7-9}-ax-H); 1.53 (1H, d, J = 12.7 Hz, sty.C_8-eqv-H); 1.60–1.78 (12H, m, adm. C_4'–H/C_6'–H/C_9'–H and sty.C_6–H/C_{10}–H/C_7-eqv-H and C_9-eqv-H); 1.85 (6H, d, J = 2.4 Hz, adm. C_2'–H/C_8'–H/C_{10}'–H); 1.98 (3H, broad s, adm. C_3'–H/C_5'–H/C_7'–H); 2.46 (5H, m, DMSO-d_6 and –CHa–COOH); 3.01 (1H, dd, J = 16.9; 3.8 Hz, CHb–COOH) 3.99 (1H, dd, J = 10.4; 3.9 Hz, C_2–H); 9.59 (1H, s, CONH); 12.60 (1H, s, COOH). ^{13}C NMR (DMSO-d_6, 500 MHz) δ (ppm): 23.19/23.52 (cyclohex. C_7/C_9); 24.51 (cyclohex. C_8); 27.97/28.00 (adm. C_3'/C_5'/C_7'); 36.41/36.48/36.55 (adm. C_4'/C_6'/C_9'); 38.63 (cyclohex. C_6/C_{10}); 38.76/38.82/38.88 (adm. C_2'/C_8'/C_{10}'); 39.21 (CH_2–COOH); 40.29 (C_1'); 40.48 (DMSO-d_6 and C_2); 71.44 (cyclohex. C_5); 168.57 (CONH); 172.19 (C_3); 176.84 (COOH); anal. calcd. for $C_{21}H_{30}N_2O_4S{\cdot}H_2O$: C, 59.41; H, 7.60; N, 6.60. Found: C, 59.43; H, 7.50; N, 6.57. ^{13}C NMR (DEPT) (500 MHz; DMSO-d_6/TMS) δ (ppm): 23.11/23.51 (C_7/C_9); 24.49 (C8); 27.51 (adm. C_3'/C_5'/C_7'); 35.99 (adm. C_4'/C_6'/C_9'); 37.48 (cyclohex. C_6/C_{10}); 38.32 (adm. C_2'/C_8'/C_{10}'); 38.67 (CH_2–COOH); 39.79 (C_1'); 39.95 (cyclohex. C_2); 70.93 (cyclohex. C_5); 168.07 (CONH); 171.68 (C_3); 176.34 (COOH).

*[4-(Adamantane-1-carboxamido)-8-methyl-3-oxo-1-thia-4-azaspiro-[4.5]decan-2-yl]acetic acid (**4c**)*

White crystals; yield: 33%; mp: 181–182°C; IR: 3489, 3118 (O–H/N–H); 2904, 2851 (C–H); 1705, 1689, 1664 (C=O); 1515 (N–H); 1452, 1368 (C–H); 1238 (N–H and C–N). ^{1}H NMR (DMSO-d_6, 500 MHz) δ (ppm): 0.85 (3H, t, J = 6.3 Hz, –CH_3); 1.01–1.28 (3H, m, sty.C_8–H, sty.C_{7-9}-ax-H); 1.61–1.80 (12H, m, adm. C_4'–H/C_6'–H/C_9'–H and sty. C_6–H/C_{10}–H/C_7-eqv-H and C_9-eqv-H); 1.85 (6H, d, J = 2.4 Hz, adm. C_2'–H/C_8'–H/C_{10}'–H); 1.98 (3H, broad s, adm. C_3'–H/C_5'–H/C_7'–H); 2.45 (5H, m, DMSO-d_6 and –CHa–COOH); 3.01 (1H, dd, J = 16.9; 3.8 Hz, –CHb–COOH) 3.99 (1H, dd, J = 10.5; 3.9 Hz, C_2–H); 9.59 (1H, s, CONH); 12.60 (1H, s, COOH). ^{13}C NMR (DMSO-d_6, 500 MHz) δ (ppm): 22.21 (CH_3); 27.91/28.06 (cyclohex. C_7/C_9); 31.04 (cyclohex. C_8); 27.97/28.00 (adm. C_3'/C_5'/C_7'); 31.04 (C_8); 36.40/36.48/36.55 (adm. C_4'/C_6'/C_9'); 38.61 (cyclohex. C_6/C_{10}); 38.75/38.81/38.87 (adm. C_2'/C_8'/C_{10}'); 39.23 (CH_2–COOH); 40.28 (C_1'); 40.49 (DMSO-d_6 and C_2); 71.30 (cyclohex. C5); 168.64 (CONH); 172.20 (C3); 176.81 (COOH); MS APCI(−) m/z (%): 419 [M−H]$^-$, MS APCI(+) m/z (%): 135 (100). Anal. calcd. for $C_{22}H_{32}N_2O_4S{\cdot}H_2O$: C, 60.25; H, 7.81; N, 6.39. Found: C, 60.35; H, 7.36; N, 6.23.

*[4-(Adamantane-1-carboxamido)-8-ethyl-3-oxo-1-thia-4-azaspiro-[4.5]decan-2-yl]acetic acid (**4d**)*

White crystals; yield: 81%; mp: 156–157°C; IR: 3481, 3117 (O–H/N–H); 2902, 2852 (C–H); 1705, 1689, 1667 (C=O); 1519 (N–H); 1443, 1367 (C–H); 1245 (N–H and C–N). ^{1}H NMR (DMSO-d_6, 500 MHz) δ (ppm): 0.84 (3H, t, J = 7.4 Hz, –CH_2CH_3); 0.96–1.13 (3H, m, sty.C_8–H, sty. C_{7-9}-ax-H); 1.13–1.28 (2H, m, –CH_2CH_3); 1.62–1.80 (12H, m, adm. C_4'-H/C_6'-H/C_9'-H and sty. C_6–H/C_{10}–H/C_7-eqv-H and C_9-eqv-H); 1.85 (6H, d, J = 2.4 Hz, adm. C_2'-H/C_8'-H/C_{10}'-H); 1.98 (3H, broad s, adm. C_3'–H/C_5'–H/C_7'–H); 2.45 (5H, m, DMSO-d_6 and –CHa–COOH); 3.01 (1H, dd, J = 16.9; 3.8 Hz, –CHb–COOH); 3.99 (1H, dd, J = 10.5; 3.9 Hz, C_2–H); 9.59 (1H, s, CONH); 12.57 (1H, s, COOH). ^{13}C NMR (DMSO-d_6, 500 MHz) δ (ppm): 11.83 (–CH_2CH_3); 29.06 (–CH_2CH_3); 29.51/29.59 (cyclohex. C_7/C_9); 37.57 (cyclohex. C_8); 27.97/28.00 (adm. C_3'/C_5'/C_7'); 36.40/36.48/36.55 (adm. C_4'/C_6'/C_9'); 38.61 (cyclohex. C_6/C_{10}); 38.75/38.81/38.87 (adm. C_2'/C_8'/C_{10}'); 39.24 (CH_2–COOH); 40.28 (C_1'); 40.48 (DMSO-d_6 and C_2); 71.60 (cyclohex. C_5); 168.62 (CONH); 172.20 (C_3); 176.79 (COOH); MS APCI(−) m/z (%): 433 [M−H]$^-$, MS APCI(+) m/z (%) 135 (100). Anal. calcd. for $C_{23}H_{34}N_2O_4S{\cdot}H_2O$: C, 61.03; H, 8.02; N, 6.19. Found: C, 61.09; H, 7.57; N, 6.14.

*[4-(Adamantane-1-carboxamido)-3-oxo-8-propyl-1-thia-4-azaspiro-[4.5]decan-2-yl]acetic acid (**4e**)*

White powder; yield: 93%; mp: 148–149°C; IR: 3482, 3110 (O–H/N–H); 2908, 2849 (C–H); 1705, 1690, 1667 (C=O); 1519 (N–H); 1442, 1367 (C–H); 1242 (N–H and C–N). ^{1}H NMR (DMSO-d_6, 500 MHz) δ (ppm): 0.85 (3H, t, J = 7.3 Hz, –$CH_2CH_2CH_3$); 0.97–1.17 (5H, m, sty.C_8–H, sty.C_{7-9}-ax-H and –$CH_2CH_2CH_3$); 1.19–1.31 (2H, m, –$CH_2CH_2CH_3$); 1.60–1.81 (12H, m, adm. C_4'–H/C_6'–H/C_9'–H and sty. C_6–H/C_{10}–H/C_7-eqv-H and C_9-eqv-H); 1.85 (6H, d, J = 2.3 Hz, adm. C_2'–H/C_8'–H/C_{10}'–H);

1.98 (3H, broad s, adm. C_3'-H/C_5'–H/C_7'–H); 2.46 (1H, dd, J = 10.5; 6.4 Hz, –CHa–COOH); 3.01 (1H, dd, J = 16.9; 3.7 Hz, CHb–COOH); 3.99 (1H, dd, J = 10.5; 3.9 Hz, C_2–H); 9.59 (1H, s, CONH); 12.61 (1H, s, COOH). ^{13}C NMR (DMSO-d_6, 500 MHz) δ (ppm): 14.65, –$CH_2CH_2CH_3$); 27.97/28.00 (adm. C_3'/C_5'/C_7'); 29.06, –$CH_2CH_2CH_3$); 29.59/29.51 (cyclohex. C_7/C_9); 36.40/36.48/36.55 (adm. C_4'/C_6'/C_9'); 38.61 (cyclohex. C_6/C_{10}); 37.56 (cyclohex. C_8); 38.74/38.81/38.87 (adm. C_2'/C_8'/C_{10}'); 38.87 (–$CH_2CH_2CH_3$); 39.24 (CH_2–COOH); 40.28 (C_1'); 40.48 (DMSO-d_6 and C_2); 71.60 (cyclohex. C_5); 168.62 (CONH); 172.20 (C_3); 176.81 (COOH); anal. calcd. for $C_{24}H_{36}N_2O_4S{\cdot}H_2O$: C, 61.77; H, 8.21; N, 6.00. Found: C, 61.87; H, 7.76; N, 5.99.

*[4-(Adamantane-1-carboxamido)-8-*tert*-butyl-3-oxo-1-thia-4-azaspiro[4.5]decan-2-yl]acetic acid (**4f**)*

White powder; yield: 69%; mp: 180°C; IR: 3496, 3119 (O–H/N–H); 2907, 2848 (C–H); 1695, 1663, 1522 (N–H); 1443, 1367 (C–H); 1240 (N–H and C–N). ^{1}H NMR (DMSO-d_6, 500 MHz) δ (ppm): 0.83 (9H, s, –C(CH_3)$_3$); 0.85–0.96 (1H, m, sty.C_8-ax-H); 1.08–1.26 (2H, m, C_{7-9}-ax-H); 1.61–1.80 (12H, m, adm. C_4'-H/C_6'-H/C_9'-H and sty.C_6–H/C_{10}–H/C_{7-9}-eqv-H); 1.85 (6H, d, 2,09 Hz, adm. C_2'-H/C_8'–H/C_{10}'–H); 1.98 (3H, broad s, adm. C_3'–H/C_5'–H/C_7'–H); 2.46 (5H, m, DMSO-d_6 and –CHa–COOH); 3.01 (1H, dd, J = 16.9; 3.7 Hz, –CHb–COOH); 3.99 (1H, dd, J = 10.5; 4.0 Hz, C_2–H); 9.59 (1H, s, CONH); 12.54 (1H, s, COOH). ^{13}C NMR (DMSO-d_6, 500 MHz) δ (ppm): 24.02/24.32 (cyclohex. C_7/C_9); 27.75 (C(CH_3)$_3$); 27.97/28.00 (adm. C_3'/C_5'/C_7'); 32.42 (C(CH_3)$_3$); 36.40/36.48/36.55 (adm. C_4'/C_6'/C_9'); 38.62 (cyclohex. C_6/C_{10}); 38.75/38.81/38.85 (adm. C_2'/C_8'/C_{10}'); 39.24 (CH_2–COOH); 40.27 (C_1'); 40.49 (DMSO-d_6 and C_2); 46.11 (cyclohex. C_8); 71.48 (cyclohex. C_5); 168.62 (CONH); 172.21 (C_3); 176.80 (COOH); MS APCI(–) m/z (%): 461 [M–H]$^-$, MS APCI(+) m/z (%): 135 (100); anal. calcd. for $C_{25}H_{38}N_2O_4S{\cdot}H_2O$: C, 62.47; H, 8.39; N, 5.83. Found: C, 62.54; H, 7.99; N, 5.70.

*[4-(Adamantane-1-carboxamido)-8-phenyl-3-oxo-1-thia-4-azaspiro-[4.5]decan-2-yl]acetic acid (**4g**)*

White powder; yield: 61%; mp: 174–175°C; IR: 3489, 3111 (O–H/N–H); 2908, 2849 (C–H); 1697, 1667, 1522 (N–H); 1442, 1367 (C–H); 1242 (N–H and C–N). ^{1}H NMR (DMSO-d_6, 500 MHz) δ (ppm): 1.54–1.74 (9H, m, adm. C_4'–H/C_6'–H/C_9'–H/C_7-eqv-H and C_9-eqv-H); 1.77–1.94 (12H, m, adm. C_2'–H/C_8'–H/C_{10}'–H; sty.C_6–H/C_{10}–H, C7-9-ax-H); 2.01 (3H, broad s, adm. C_3'–H/C_5'–H/C_7'–H); 2.41–2.55 (6H, m, DMSO-d_6 ile sty.C8-ax-H and –CHa–COOH); 3.05 (1H, dd, J = 1.9; 3.7 Hz, –CHb–COOH); 4.06 (1H, dd, J = 10.5; 3.8 Hz, C_2–H); 9.67 (1H, s, CONH); 12.63 (1H, s, COOH). ^{13}C NMR (DMSO-d_6, 500 MHz) δ (ppm): 27.99/28.01 (adm. C_3'/C_5'/C_7'); 30.74/31.19 (cyclohex. C_7/C_9); 36.43/36.50/36.57 (adm. C_4'/C_6'/C_9'); 38.63 (cyclohex. C_6/C_{10}); 38.79/38.84/38.90 (adm. C_2'/C_8'/C_{10}'); 39.30 (CH_2–COOH); 40.31 (C_1'); 40.48 (DMSO-d_6 and C_2); 41.97 (cyclohex. C_8); 71.02 (cyclohex. C_5); 126.63 C_4(Ph); 127.98, C_2(Ph)/C_6(Ph); 128.88/128.74 C_3(Ph)/C_5(Ph); 146.37 C_1(Ph); 168.66 (CONH); 172.23 (C_3); 176.92 (COOH); anal. calcd. for $C_{27}H_{34}N_2O_4S{\cdot}H_2O$: C, 64.77; H, 7.25; N, 5.60. Found: C, 64.88; H, 6.90; N, 5.45.

4.2 | Pharmacological/biological assays

4.2.1 | Cell culture and cytotoxicity

The cytotoxicity of the newly synthesized compounds was evaluated by the MTT assay using the human hepatocellular carcinoma (HepG2, HB-8065™), human prostate adenocarcinoma (PC-3, CRL-1435™), human lung carcinoma (A549, CCL-185™), and mouse fibroblast cell lines (NIH/3T3, CRL-1658™). Cell lines were obtained from the American Type Culture Collection (ATCC). Cells were incubated in Dulbecco's modified Eagle's medium/Nutrient Mixture F-12 (DMEM/F-12; Wisent Bioproducts) with 10% fetal bovine serum and antibiotics (1% penicillin, 1% streptomycin) in 95% O_2 and 5% CO_2 at 37°C. The monolayer cells grown to 80–85% confluency were detached with trypsin. The MTT assay evaluates the viability of cells by the reduction of yellow tetrazolium salt (MTT) via a mitochondrial-dependent reaction to form an insoluble purple formazan crystal.[55,56] Furthermore, 1×10^4 cells in 100 µl medium in each well were seeded into a 96-well plate and incubated at 37°C (5% CO_2) for 24 h to allow for cell attachment. After 24 h, the cells were treated with serial concentrations of the test compounds in the range of 31.25–1000 µg/ml. Test compounds were dissolved in DMSO. After dilutions, cells in each well were treated with six different concentrations of each compound. The medium containing no sample (growth control), 0.1% sodium dodecyl sulfate (positive control), and 1% DMSO (solvent control) served as the controls. Doxorubicin was used as a positive control in the concentration range of 3.125–100 µM. For all concentrations, it was tested in triplicates and each test was repeated twice. Assay and evaluations of results were performed as described previously.[57]

4.2.2 | Analysis of apoptosis by flow cytometry

Apoptosis detection was evaluated using APC Annexin V Apoptosis Detection Kit with PI (BioLegend Inc.) by flow cytometry (Acea Novocyte 1000) in A549 cells according to manufacturer's instructions. In brief, A549 cells were seeded on a 24-well plate at a density of 5×10^4 cells/well for 24 h at 37°C for adherence and then treated with IC_{50} of **4a–c** compounds. Following a 24-h treatment, the cells were trypsinized, washed twice in cold phosphate-buffered saline, and resuspended in binding buffer. Then, the cells were incubated in the dark with 5 µl of Annexin V-FITC and 5 µl of PI for 15 min. After incubation, 400 µl of annexin-binding buffer was added, and the samples were analyzed by flow cytometry. The experiment was repeated three times and the data presented are the average values (%) compared with the control group.

4.2.3 | Quantitative real-time polymerase chain reaction analysis of apoptosis genes

A549 cells were treated with the IC_{50} concentrations of the selected **4a–c** compounds. After incubation for 24 h, total RNA was

TABLE 3 Primers used in real-time polymerase chain reaction analysis of selected apoptosis genes and the corresponding annealing temperatures

Gene	Primer sequences (5′–3′)	T_a (°C)	References
p53	F: AGAGTCTATAGGCCCACCCC R: GCTCGACGCTAGGATCTGAC	61	[6]
CASP3	F: GCTATTGTAGGCGGTTGT R: TGTTTCCCTGAGGTTTGC	53	[6]
CASP9	F: ACCAGAGATTCGCAAACCAG R: TCACCAAATCCTCCAGAACC	57	[58]
BCL2	F: TGTGGCCCAGATAGGCACCCAG R: ACTTCGCCGAGATGTCCAGCCAG	66	[6]
BAX	F: ACCAAGAAGCTGAGCGAGTATC R: ACAAAGATGGTCACGGTCTGCC	61	[6]
CYCS	F: CTTACACAGCCGCCAATA R: CTTCTTCTTAATGCCGACAA	53	[59]
AIF	F: TGCTGGTGGACATGAAGGAC R: TTTGGCGAACCCTGTCTCC	59	[58]
APAF1	F: CCTCCAAAAACCCAGCCAAC R: TCCAGGACCCTGGGGATTTC	61	[60]
XIAP	F: ACTCTACTACACAGGTATTGG R: TCAGAACTCACAGCATCAG	55	[61]
β-Actin	F: AACTACCTTCAACTCCAT R: TGATCTTGATCTTCATTGTG	48	[62]

extracted from control and **4a**-, **4b**-, and **4c**-treated groups in A549 cell lines using a High Pure RNA Isolation Kit (Roche Life Sciences) according to the instructions provided by the manufacturer. Complementary DNA (cDNA) was synthesized using the mixture of anchored oligo(dT) and random hexamer primers by Transcriptor First Strand cDNA Synthesis Kit (Roche Life Sciences). Gene expression levels of apoptosis genes including *p53*, *CASP3*, *CASP9*, *BCL2*, *BAX*, *CYCS*, *AIF*, *APAF1*, and *XIAP* were measured using BioLine SensiFast™ Syber® No-Rox Kit on LightCycler® 480 Instrument II (Roche Life Science). The primer sequences and their annealing temperatures of the genes are provided in Table 3 (Sentromer DNA Technologies). The gene expression analysis and evaluations of results for all genes were performed as described previously.[57]

4.2.4 | Statistical analysis

Results of cytotoxicity, apoptosis assay, and gene expression analysis levels were represented as mean ± *SD*. Statistical analysis was performed by analysis of variance, followed by Dunnett's multiple comparison test using "SPSS version 21.0 for Windows," statistical program (IBM Analytics). $p < .05$ and $p < .001$ were selected as the levels of significance.

4.3 | Molecular calculations

4.3.1 | Modeling

BIR3 domain of human *XIAP* was obtained from Smac bound X-ray structure with 2.0 Å resolution (PDB ID: 1G73).[63] Smac and water molecules were removed, whereas Zn^{2+} ion was retained. This XIAP structure was used as an initial structure for the relaxation of the protein through molecular dynamics (MD) simulations.

Compounds **4a–c** were sketched using Marvin Sketch 15.12.14 software.[64] Geometry optimization of the compounds was performed using YASARA Structure software[65] with NOVA force field.[66] These structures were used for molecular docking.

4.3.2 | Molecular docking

The equilibrated *XIAP* protein structure was obtained from 20-ns-long MD simulation, whose details are discussed below. Then, rigid receptor and flexible ligand docking were performed on YASARA Structure software, which utilized AutoDock Vina software.[67] Docking space (grid) was limited to a searching space, which was created with 8.0 Å distance around all atoms of the protein, yielding a cubic box with dimensions 54 × 54 × 54 Å. Binding affinities reported in the paper were obtained from molecular docking calculations.

4.3.3 | Molecular dynamics simulations

MD simulations of ligands bound to XIAP protein were performed using YASARA2 force field, as implemented in the YASARA Structure software. The box was filled with single point charge water molecules.[68] The protein–ligand complex was placed into a box with dimensions of 54 × 54 × 54 Å. The boundary of the simulated box was conditioned in the periodic form. The water density was set at 0.997 g/ml at a temperature of 303 K. The simulation was run for 20 ns.

ACKNOWLEDGMENT

The present work was supported by the Istanbul University Scientific Research Projects (Project No: TYL-2017-25681).

CONFLICTS OF INTERESTS

The authors declare that there are no conflicts of interests.

ORCID

Fusun Goktas http://orcid.org/0000-0003-2412-2232

REFERENCES

[1] F. Bray, J. Ferlay, I. Soerjomataram, R. L. Siegel, L. A. Torre, A. Jemal, *CA Cancer J. Clin.* **2018**, *68*, 394. https://doi.org/10.3322/caac.21492
[2] R. S. Y. Wong, *J. Exp. Clin. Cancer Res.* **2011**, *30*, 87. https://doi.org/10.1186/1756-9966-30-87
[3] D. Hanahan, R. A. Weinberg, *Cell J.* **2000**, *100*, 57. https://doi.org/10.1016/S0092-8674(00)81683-9
[4] D. Hanahan, R. A. Weinberg, *Cell J.* **2011**, *144*, 646. https://doi.org/10.1016/j.cell.2011.02.013
[5] Y. C. Duan, Y. C. Zheng, X. C. Li, M. M. Wang, X. W. Ye, Y. Y. Guan, G. Z. Liu, J. X. Zheng, H. M. Liu, *Eur. J. Med. Chem.* **2013**, *64*, 99. https://doi.org/10.1016/j.ejmech.2013.03.058
[6] A. G. Ali, M. F. Mohamed, A. O. Abdelhamid, M. S. Mohamed, *Bioorg. Med. Chem.* **2017**, *25*, 241. https://doi.org/10.1016/j.bmc.2016.10.040
[7] L. Wanka, K. Iqbal, P. R. Schreiner, *Chem. Rev.* **2013**, *11*, 33516. https://doi.org/10.1021/cr100264t
[8] S. D. C. Griffin, L. P. Beales, D. S. Clarke, O. Worsfold, S. D. Evans, J. Jaeger, M. Harris, D. J. Rowlands, *FEBS Lett.* **2003**, *535*, 34. https://doi.org/10.1016/S0014-5793(02)03851-6
[9] I. Stylianakis, A. Kolocouris, N. Kolocouris, G. Fytas, G. B. Foscolos, E. Padalko, J. Neyts, E. De Clercq, *Bioorg. Med. Chem. Lett.* **2003**, *13*, 1699. https://doi.org/10.1016/S0960-894X(03)00231-2
[10] K. N. Chuchkov, R. K. Georgivev, G. Ivanova, A. S. Galabov, I. G. Stankova *Proc. Fifth Int. Sci. Conf. FMNS2013.* **2013**, *4*, pp. 1–274.
[11] F. Göktaş, E. Vanderlinden, L. Naesens, N. Cesur, Z. Cesur, *Bioorg. Med. Chem.* **2012**, *20*, 7155. https://doi.org/10.1016/j.bmc.2012.09.064
[12] H. Hu, C. Lin, M. Ao, Y. Ji, B. Tang, X. Zhou, M. Fang, J. Zeng, Z. Wu, et al, *R. Soc. Chem. Adv.* **2017**, *7*, 51640. https://doi.org/10.1039/c7ra08149a
[13] A. Orzeszko, B. Kamińska, G. Orzeszko, B. J. Starościak, *Farmaco* **2000**, *55*, 619. https://doi.org/10.1016/S0014-827X(00)00075-6
[14] A. Orzeszko, B. Kamińska, B. J. Starościak, *Farmaco* **2002**, *57*, 619. https://doi.org/10.1016/S0014-827X(02)01199-0
[15] D. A. Plachta, A. M. Baranowski, A. E. Laudy, B. J. Starościak, J. Kleps, *Acta Pol. Pharm.* **2007**, *64*, 535.
[16] C. Tratrat, M. Haroun, A. Paparisva, A. Geronikaki, Ch. Kamoutsis, A. Ćirić, J. Glamočlija, M. Soković, Ch. Fotakis, P. Zoumpoulakis, S. S. Bhunia, *Arabian Journal of Chemistry* **2018**, *11*, (*4*), 573–590. https://doi.org/10.1016/j.arabjc.2016.06.007
[17] A. A. Kadi, N. R. El-Brollosy, O. A. Al-Deeb, E. E. Habib, T. M. Ibrahim, A. A. El-Emam, *Eur. J. Med. Chem.* **2007**, *42*, 235. https://doi.org/10.1016/j.ejmech.2006.10.003
[18] V. S. Georgiev. *US Patent 4,549,014*, **1985**.
[19] I. Papanastasiou, A. Tsotinis, N. Kolocouris, S. R. Prathalingam, J. M. Kelly, *J. Med. Chem.* **2008**, *51*, 1496. https://doi.org/10.1021/jm7014292
[20] W. Danysz, C. G. Parsons, J. Kornhuber, W. J. Schmidt, G. Quack, *Neurosci. Biobehav. Rev.* **1997**, *21*, 455. https://doi.org/10.1016/S0149-7634(96)00037-1
[21] S. Kumar, H. Kaur, K. K. Saxena, M. Sharrna, P. Vishwakarma, A. Kumar, *Indian. J. Chem. Sect. B.* **2010**, *49B*, 1398. https://doi.org/10.1002/chin.201110114
[22] V. S. C. Yeh, J. R. Patel, H. Yong, R. Kurukulasuriya, S. Fung, K. Monzon, W. Chiou, J. Wang, D. Stolarik, H. Imade, D. Beno, M. Brune, P. Jacobson, H. Sham, J. T. Link, *Bioorg. Med. Chem. Lett.* **2006**, *16*, 5414. https://doi.org/10.1016/j.bmcl.2006.07.055
[23] B. Sorensen, J. Rohde, J. Wang, S. Fung, K. Monzon, W. Chiou, L. Pan, X. Deng, D. Stolarik, E. U. Frevert, P. Jacobson, J. T. Link, *Bioorg. Med. Chem. Lett.* **2006**, *16*, 5958. https://doi.org/10.1016/j.bmcl.2006.08.129
[24] A. A. Spasov, T. V. Khamidova, L. I. Bugaeva, I. S. Morozov, *Pharm. Chem. J.* **2000**, *34*, 3. https://doi.org/10.1007/BF02524549
[25] S. L. Rolewski, *Dermatol. Nurs.* **2003**, *15*, 447.
[26] D. J. Augeri, J. A. Robl, D. A. Betebenner, D. R. Magnin, A. Khanna, J. G. Robertson, A. Wang, L. M. Simpkins, P. Taunk, Q. Huang, S. P. Han, B. Abboa-Offei, M. Cap, L. Xin, L. Tao, E. Tozzo, G. E. Welzel, D. M. Egan, J. Marcinkeviciene, S. Y. Chang, S. A. Biller, M. S. Kirby, R. A. Parker, L. G. Hamann, *J. Med. Chem.* **2005**, *48*, 5025. https://doi.org/10.1021/jm050261p
[27] C. Mathieu, E. Degrande, *Vasc. Health Risk Manage.* **2008**, *4*, 1349.
[28] D. E. Ickes, T. M. Venetta, Y. Phonphok, K. S. Rosenthal, *Antiviral Res.* **1990**, *14*, 75. https://doi.org/10.1016/0166-3542(90)90045-9
[29] J. Dwivedi, K. Devi, Y. Asmat, S. Jain, S. Sharma, *J. Saudi Chem. Soc.* **2016**, *20*, 16. https://doi.org/10.1016/j.jscs.2012.09.001
[30] K. R. Raju, A. R. G. Prasad, B. S. Kumar, L. K. Ravindranath, *J. Chem. Technol. Metall.* **2014**, *49*, 238. https://doi.org/10.5457/328
[31] D. Kaminskyy, D. Khyluk, O. Vasylenko, L. Zaprutko, R. Lesyk, *Sci. Pharm.* **2011**, *79*, 763. https://doi.org/10.3797/scipharm.1109-14
[32] Ö. Güzel, N. Terzioğlu, G. Çapan, A. Salman, *Arkivoc* **2006**, *12*, 98. https://doi.org/10.3998/ark.5550190.0007.c12
[33] V. Opletalova, J. Dolezel, J. Kunes, V. Buchta, M. Vejsova, M. Kucerova-Chlupacova, *Molecules* **2016**, *21*, 1592. https://doi.org/10.3390/molecules21111592
[34] F. Göktaş, E. Vanderlinden, L. Naesens, Z. Cesur, N. Cesur, P. Taş, *Phosphorus, Sulfur Silicon Relat. Elem.* **2015**, *190*, 1075. https://doi.org/10.1080/10426507.2014.965819
[35] V. P. Peroković, Ž. Car, A. Usenik, T. Opačak-Bernardi, A. Jurić, S. Tomić, *Mol. Divers.* **2020**, *24*, 253. https://doi.org/10.1007/s11030-019-09948-1
[36] A. A. Al-Mutairi, M. A. Al-Alshaikh, F. A. M. Al-Omary, H. M. Hassan, A. M. El-Mahdy, A. A. El-Emam, *Molecules* **2019**, *24*, 4308. https://doi.org/10.3390/molecules24234308
[37] V. H. Pham, T. P. D. Phan, D. C. Phan, B. D. Vu, *Molecules* **2020**, *25*, 324. https://doi.org/10.3390/molecules25020324
[38] D. F. Aguiar, L. L. A. Dutra, W. M. Dantas, *ChemistrySelect* **2019**, *4*, 9112. https://doi.org/10.1002/slct.201901285
[39] N. A. Zefirov, E. V. Nurieva, Y. A. Pikulina, A. V. Ogon´kov, B. Wobith, S. A. Kuznetsov, O. N. Zefirova, *Russ. Chem. Bull., Int. Ed.* **2017**, *66*, 1503.
[40] W. Hu, X. S. Huang, J. F. Wu, L. Yang, Y. T. Zheng, Y. M. Shen, Z. Y. Li, X. Li, *J. Med. Chem.* **2017**, *61*, 8947. https://doi.org/10.1021/acs.jmedchem.7b01202
[41] A. Letai, *Annu. Rev. Cancer Biol.* **2017**, *1*, 275. https://doi.org/10.1146/annurev-cancerbio-050216-121933

[42] Z. Chen, J. Li, X. Song, Z. Wang, W. Yue, *Exp. Ther. Med.* **2012**, *3*, 273. https://doi.org/10.3892/etm.2011.390
[43] T. Chen, Y. S. Wong, *Int. J. Biochem. Cell Biol.* **2009**, *41*, 666. https://doi.org/10.1016/j.biocel.2008.07.014
[44] S. Y. Jeong, M. H. Han, C. Y. Jin, B. T. Choi, T. J. Nam, S. K. Kim, Y. H Choi et al., *Int. J. Mol. Med.* **2010**, *25*, 31. https://doi.org/10.3892/ijmm_00000310
[45] D. Bose, S. Banerjee, S. Das, N. Chatterjee, K. D. Saha, *Cell. Physiol. Biochem.* **2016**, *38*, 1303. https://doi.org/10.1159/000443125
[46] R. Agarwal, S. B. Kaye, *Nat. Rev. Cancer* **2003**, *3*, 502. https://doi.org/10.1038/nrc1123
[47] S. I. Abdel Wahab, A. B. Abdul, A. S. Alzubairi, M. Mohamed Elhassan, S. Mohan, *J. Biomed. Biotechnol.* **2009**, *2009*, 1. https://doi.org/10.1155/2009/769568
[48] J. Lu, D. McEachern, H. Sun, L. Bai, Y. Peng, S. Qiu, R. Miller, J. Liao, H. Yi, M. Liu, A. Bellail, C. Hao, S. Y. Sun, A. T. Ting, S. Wang, *Mol. Cancer Ther.* **2011**, *10*, 902. https://doi.org/10.1158/1535-7163.MCT-10-0864
[49] A. D. Schimmer, *Cancer Res.* **2004**, *64*, 7183. https://doi.org/10.1158/0008-5472.CAN-04-1918
[50] H. S. Hofmann, A. Simm, A. Hammer, R. E. Silber, B. Bartling, *J. Cancer Res. Clin. Oncol.* **2002**, *128*, 554. https://doi.org/10.1007/s00432-002-0364z
[51] Y. Hu, G. Cherton-Horvat, V. Dragowska, S. Baird, R. G. Korneluk, J. P. Durkin, L. D. Mayer, E. LaCasse et al., *Clin. Cancer Res.* **2003**, *9*, 2826.
[52] N. Lalaoui, D. L. Vaux, *F1000Res.* **2018**, *7*, 1. https://doi.org/10.12688/f1000research.16439.1
[53] A. P. Marchand, D. Xing, S. G. Bott, *Tetrahedron* **1996**, *52*, 825. https://doi.org/10.1016/0040-4020(95)00934-5
[54] A. Al-Aboudi, R. A. Al-Qawasmeh, A. Shahwan, U. Mahmood, A. Khalid, Z. Ul-Haq, *Acta Pharmacol. Sin.* **2015**, *36*, 879. https://doi.org/10.1038/aps.2014.173
[55] T. Mosmann, *J. Immunol. Methods* **1983**, *65*, 55. https://doi.org/10.1016/0022-1759(83)90303-4
[56] M. C. Alley, D. A. Scudiero, A. Monks, M. L. Hursey, M. J. Czerwinski, D. L. Fine, B. J. Abbott, J. G. Mayo, R. H. Shoemaker, R. B. Michael et al., *Cancer Res.* **1988**, *48*, 589.
[57] E. F. Karaman, S. Ozden, *Mycotoxin Res.* **2019**, *35*, 309. https://doi.org/10.1007/s12550-019-00358-8
[58] A. de Souza Prestes, M. M. dos Santos, A. Ecker, G. T. de Macedo, R. Fachinetto, G. N. Bressan, J. da Rocha, N. V. Barbosa, *Toxicol. In Vitro* **2019**, *55*, 33. https://doi.org/10.1016/j.tiv.2018.11.001
[59] Zhou Xiao-Tao, Pu Ze-Jin, Liu Li-Xuan, Li Guo-Ping, Feng Jia-Lin, Zhu Hua-Chen, Wu Ling-Fei, Inhibition of autophagy enhances adenosine-induced apoptosis in human hepatoblastoma HepG2 cells *Oncology Reports* **2018**. https://doi.org/10.3892/or.2018.6899
[60] Y. S. Zang, Y. F. Zhong, Z. Fang, B. Li, J. An, *Cancer Gene Ther.* **2012**, *19*, 773. https://doi.org/10.1038/cgt.2012.60
[61] D. Yin, N. Wang, S. Zhang, Y. Jiang, Y.-m Lu, H. Wei, N.-c Huo, Q. Xiao, Y.-l Ou, *Cell Biochem. Biophys.* **2014**, *71*, 161. https://doi.org/10.1007/s12013-014-0179-y
[62] Rosa Susana C, Gonçalves Juliana, Judas Fernando, Mobasheri Ali, Lopes Celeste, Mendes Alexandrina F, Impaired glucose transporter-1 degradation and increased glucose transport and oxidative stress in response to high glucose in chondrocytes from osteoarthritic versus normal human cartilage *Arthritis Research & Therapy* **2009**, *11*, (*3*), R80. https://doi.org/10.1186/ar2713
[63] G. Wu, J. Chai, T. L. Suber, J. W. Wu, C. Du, X. Wang, Y. Shi, *Nature* **2000**, *400*, 1008.
[64] Marvin was used for drawing, displaying and characterizing chemical structures, substructures and reactions, Marvin 15.12.14, ChemAxon. http://www.chemaxon.com
[65] E. Krieger, G. Vriend, Models@Home: Distributed Computing in Bioinformatics Using a Screensaver Based Approach. Vol 18; 2002. www.mosix.cs.huji.ac.il (accessed: April 2020).
[66] E. Krieger, G. Koraimann, G. Vriend, *Proteins* **2002**, *47*, 393. https://doi.org/10.1002/prot.10104
[67] O. Trott, A. J. Olson, *J. Comput. Chem.* **2009**, *31*, 455. https://doi.org/10.1002/jcc.21334
[68] P. E. Smith, W. F. Van Gunsteren, *Chem. Phys. Lett.* **1993**, *215*, 315. https://doi.org/10.1016/0009-2614(93)857209

SUPPORTING INFORMATION

Additional Supporting Information may be found online in the supporting information tab for this article.

How to cite this article: Turk-Erbul B, Karaman EF, Duran GN, Ozbil M, Ozden S, Goktas F. Synthesis, in vitro cytotoxic and apoptotic effects, and molecular docking study of novel adamantane derivatives. *Arch Pharm.* 2021;354:e2000256. https://doi.org/10.1002/ardp.202000256